Electrical Discharge in Capillary Breakup: Controlling the Charge of a Droplet

Jean-Christophe Baret
Philips Research Laboratories Eindhoven, Prof. Holstlaan 4, 5656AA Eindhoven, The Netherlands

Frieder Mugele*
University of Twente, PO Box 217, 7500AE Enschede, The Netherlands

(Received 21 July 2005; published 10 January 2006)

We studied the detachment of sessile droplets of conductive liquids from an immersed wire by reducing the contact angle using ac electrowetting. Upon detachment, the droplets acquire a certain amount of charge, which is shown to be controlled by a dimensionless parameter α. α describes the interplay between the diverging Ohmic resistance of the breaking capillary neck and the ac frequency. In the specific configuration of the present experiment, discharging at high frequency leads to self-excited oscillations in which the droplets periodically detach from and reattach to the wire.

DOI: 10.1103/PhysRevLett.96.016106 PACS numbers: 68.03.−g, 68.05.−n, 83.60.Np

The manipulation of tiny amounts of liquids has become a paradigm in various fields of applied physics such as printing and coating technology or biotechnology related microfluidics. Pressure gradients for driving fluid motion are traditionally generated using mechanical, thermomechanical, or electrical actuators. Given the intrinsically high surface to volume ratio in microfluidics, on-demand variations of interfacial energies such as thermocapillary effects [1] and electrowetting [2] have received increasing attention in recent years. The interplay of surface tension and electric fields can also be used to generate liquid jets [3] and droplets, for example in electrospray ionization [4,5] or in continuous ink-jet printing [6]. The role of the electric field in these examples is twofold: on the one hand, it drives the instability leading to the generation and detachment of microdroplets from the reservoir. On the other hand, it is responsible for the charge acquired by the detached droplets. In common configurations using dc voltage both aspects are tightly coupled. In the present Letter, we use low frequency ac electrowetting to detach liquid droplets from an electrode. We will show that the amount of charge acquired by a droplet detaching can be controlled by tuning the electrical properties of the liquid and the applied ac frequency. In this process, the breakup of the capillary neck in the late stage of the detachment process plays a crucial role. In conjunction with the finite conductivity of typical aqueous liquids, the algebraic decrease of the neck diameter [7,8] gives rise to a continuous divergence of the neck's Ohmic resistance. The speed of this divergence compared to the ac frequency determines to what extent the detaching droplet can be discharged.

Droplets of a conductive liquid (volume ≈ 1 μl, various mixtures of deionized water, glycerol, and NaCl) were deposited on conductive substrates that are covered by a thin insulating layer and a hydrophobic top coating (1 μm thick thermally grown SiO_2 covered by a hydrophobic self-assembled monolayer of Octadecyltrichlorosilane [9]). The composition of the liquid was varied to cover a range of viscosities η and conductivities σ from 2 mPa s to 70 mPa s and from 0.1 to 10 mS/cm, respectively. The entire system was immersed in a silicone oil bath (Fluka, viscosity $\eta = 5$ mPa s) in order to reduce both contact angle hysteresis and the influence of gravity. High-speed video images with a maximum frame rate up to 16 000 fps were recorded using a high-speed video camera (Photron fastcam ultima 512). Upon applying an ac voltage U_0 ranging from 0 to 100 V (rms at frequencies $f =$ 1–20 kHz) between the substrate and a platinum wire (electrode radius $r_e = 125$ μm) immersed into droplet, the apparent contact angle $\theta_L(U_0)$ decreased following the well-known electrowetting equation [2]:

$$\cos\theta_L(U_0) = \cos\theta_Y + \frac{c}{2\gamma} U_0^2, \tag{1}$$

where $\theta_Y = \theta_L(U_0 = 0)$ is Young's contact angle ($\approx$155 deg for water) and $c = \varepsilon_0\varepsilon_r/T$ is the droplet-substrate capacitance per unit area. γ is the surface tension of the liquid in the surrounding fluid ($\gamma = 38$ mN/m for pure water vs silicone oil). ε_r and T are the dielectric constant and the thickness of the insulating layer, respectively, and ε_0 the electric susceptibility of vacuum.

Equation (1) holds for a droplet with a well-defined potential. If instead an electrically isolated droplet with a fixed charge q is considered, the equilibrium contact angle reads

$$\cos\theta_L(q) = \cos\theta_Y + \frac{q^2}{2CA_{\mathrm{sl}}\gamma}, \tag{2}$$

where A_{sl} is the solid-droplet interfacial area and $C_{\mathrm{sl}} = cA_{\mathrm{sl}}$ is the total capacitance. Equation (2) implies that the charge of an isolated droplet can be determined from its contact angle.

In the present experiments we placed the electrode at a distance d from the solid substrate such that it was barely immersed into the drop at zero voltage (see Fig. 1). Upon

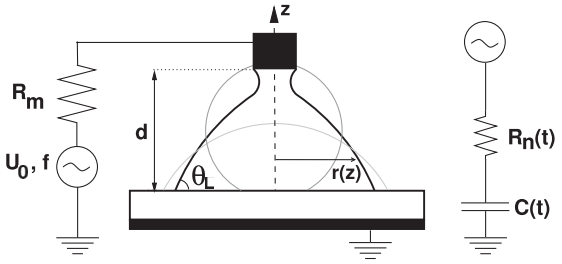

FIG. 1. Electrowetting setup with schematic droplet morphologies (not to scale) and electrical equivalent circuit. The current is measured via the resistor $R_m = 10$ kΩ.

increasing the voltage the contact angle and thus the height of the drop decreases following Eq. (1), eventually leading to the formation of a capillary neck. At a certain d-dependent critical voltage the capillary neck becomes unstable and breaks. The value of this critical voltage can be derived from Rayleigh's argument that the neck becomes unstable when its height is of the order of its circumference [10]. Based on this criterion and on additional geometric considerations, a morphological diagram can be constructed which gives the ranges of stability for both the attached and the detached droplet morphologies as a function of d and U_0. In analogy with the case of capillary bridges between parallel plates [11,12], we find that there is a region within the d-U_0 plane in which both morphologies are unstable and the droplet oscillates periodically between the attached and the detached state [13].

Here we are interested in the charge acquired by the droplet as it detaches from the electrode. Depending on the applied ac frequency and the conductivity of the liquid we observe two distinct behaviors. At low ac frequency or high conductivity (regime I) the contact angle after detachment [at $t = 0$ in Fig. 2(a)] remains close to its low value [corresponding to Eq. (1)], except for a minor increase [Fig. 2(a)]. (The size of this minor step varies from detachment event to detachment event.) Subsequently, θ increases gradually on a time scale of tens of seconds. This regime is easily understood by considering the extreme case of detachment at dc voltage: immediately after detachment the droplet has a charge $q_0 = CU_0$, which gives rise to the same contact angle as prior to the detachment [cf. Eqs. (1) and (2)]. (For the 1 kHz data in Fig. 2 we find $q \approx 0.9q_0$.) The subsequent gradual increase is due to a slow discharge via leakage currents [12]. In contrast, at high ac frequency and/or low conductivity (regime II) a substantially higher and perfectly reproducible value of θ is found within a few ms after detachment. As a consequence of this abrupt change in the boundary condition, the contact line begins to move (at a speed up to several tens of mm/s) and the droplet relaxes back towards a spherical cap with a higher contact angle within $\approx$10 ms to $\approx$100 ms depending on the viscosity and the drop size. During this relaxation the droplet reconnects to the electrode [at $t \approx$ 12 ms in Fig. 2(a)]. Once reconnected, the contact angle decreases and the droplet begins to spread again until the capillary neck breaks once more and the oscillation cycle starts all over again. The sharp increase in contact angle indicates that the droplet charge decreases substantially during detachment. Inserting the value of θ in Eq. (2), we find $q \approx 0.25q_0$. This value should be considered an upper limit: during the oscillation we can only measure the dynamic contact angle which is known to be lower than the equilibrium value for a receding contact line. In order to determine the charge more quantitatively, we measured the current in the system (Fig. 3). In the connected state (t_i0), there is a large capacitive current I due to the capacitance between the droplet and the substrate (cf. Fig. 1), whereas in the disconnected state I is essentially zero. In regime I, the current retains its full amplitude and drops to zero upon detachment rather abruptly [Fig. 3(a)]. In regime II, however, the current amplitude decreases continuously to zero over several oscillation periods [Fig. 3(b)].

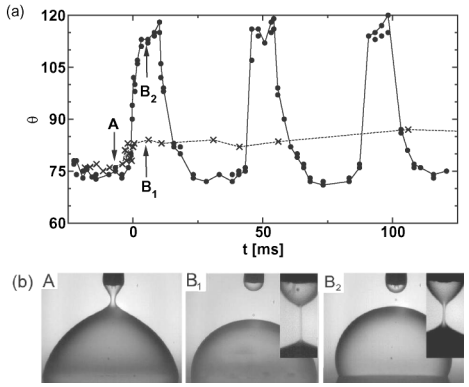

FIG. 2. (a) Contact angle vs time for $f = 1$ kHz (×) and 10 kHz (●) showing the two regimes. (b) Pictures of the drop: 1 ms before breakup (A) and 5 ms after breakup (regime I: B_1, regime II: B_2). The diameter of the electrode is 250 μm [22].

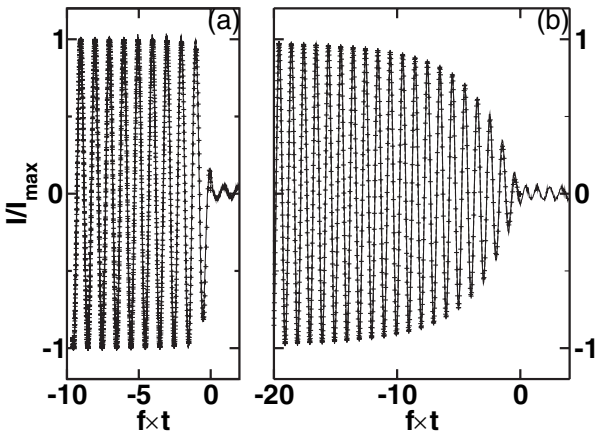

FIG. 3. Electrical current vs time close to breakup. Solid lines: experimental data; +: fit curves based on Eq. (4). (a) 1 kHz (regime I): $\alpha = 1.3$, $\mu = 1$, (b) 10 kHz (regime II): $\alpha = 5.5$, $\mu = 1$.

The droplet charge can be obtained by integrating these curves. While the result for regime I depends strongly on the phase ϕ of the ac voltage at $t = 0$, the continuous decrease in regime II always leads to discharging independent of ϕ. To understand the physics of the discharging mechanism, we note first that the time constant RC in the electrical equivalent circuit in Fig. 1 diverges because the resistance $R_n = R(t)$ of the capillary neck diverges as the pinch off is approached. As soon as $RC \geq f^{-1}$ the droplet charge cannot follow the applied ac voltage anymore. Whether the detaching droplet will be discharged or not depends on how much time (in units of f^{-1}) is left until the ultimate break off.

Before solving the differential equation of the driven RC circuit in Fig. 1 for the charge we need to analyze the divergence of $R(t)$ [14]. $R(t)$ is determined by the electrical conductivity of the liquid and by the time-dependent geometry of the capillary neck. Within a few percent accuracy it is given by [15,16]

$$R(t) = \int_{z=z_0}^{z=d} \frac{\mathrm{d}z}{\sigma \pi r(z,t)^2}, \tag{3}$$

where z_0 denotes the lower edge of a suitably chosen box of width $2r_e$ around the capillary neck [approximately the size of the insets in Fig. 2(b)]. The result is shown in Fig. 4 [17]. On the time scale of interest for the electrical discharge ($\approx$0.1–1 ms), the divergence can be reasonably well approximated by a power law $R(t) = R_0(t/t_0)^{-\mu}$ with $1 < \mu < 1.5$, where $R_0 = (\sigma r_e)^{-1}$ is the characteristic initial neck resistance and $t_0 \approx 0.5$ ms is the characteristic hydrodynamic time scale for the breakup [18]. This is indeed expected on the basis of earlier studies on the

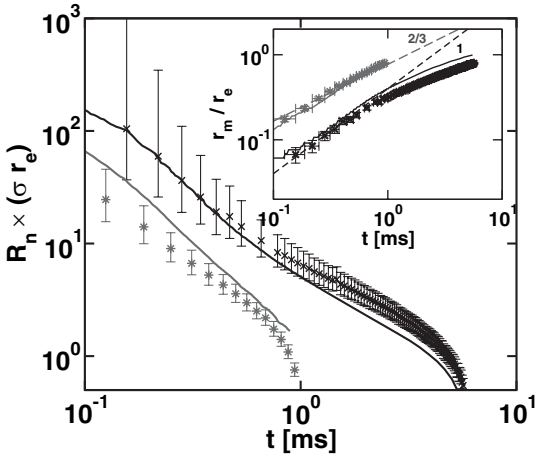

FIG. 4. Capillary neck resistance vs time prior to breakup. Symbols: experimental data ($f = 10$ kHz; *: $\eta = 2$ mPa s; $\times$: $\eta = 70$ mPa s). Solid lines: numerical computational fluid dynamics (CFD) calculations (CFD-ACE + package). Inset: minimum radius vs time. Symbols: experimental data; solid lines: CFD calculations; dashed lines: theoretical expectations for an inviscid outer fluid ($\nu = 2/3$ and $\nu = 1$ for the inertial and the viscous case, respectively).

singularity of breaking capillary necks [7,8,19,20]. It was shown that the surface profiles are self similar and that the minimal radius r_m of the capillary neck vanishes algebraically, i.e., $r_m \propto t^{\nu}$. Depending on whether inertia or viscosity is the dominant force opposing the driving capillary forces, $\nu = 2/3$ or $\nu = 1$, respectively, is found. For a few simple neck geometries, the connection between ν and μ can be given explicitly: for a cylindrical neck with constant length $R \propto r_m^{-2}$, i.e., $\mu = 2\nu$. For a cylindrical neck with a length scaling $\propto t^{1/2}$ [21] we have $\mu = 2\nu - 1/2$; for a cone-shaped geometry $\mu = \nu$ [15,16]. The two latter scenarios suggest a possible value of μ between $2/3$ and $3/2$. However, both ν and the characteristic shape can vary during a transition, allowing for various crossovers [8]. The inset of Fig. 4 shows the typical crossover from the initial inertia-dominated to the late viscosity-dominated regime around $t = 1$ ms for the high viscosity droplet. (For the low-viscosity droplet, this transition is expected to occur at shorter times.)

While the exact value of μ thus depends on various details, we will show now that the discharging mechanism itself is rather robust. Taking $R = R_0(t/t_0)^{-\mu}$ in series with the constant capacitance C, the differential equation for the dimensionless charge $Q = q/CU_0$, and in terms of the dimensionless time $\tilde{t} = 2\pi f t$ reads

$$\alpha^{1+\mu}\tilde{t}^{-\mu}\frac{\mathrm{d}Q}{\mathrm{d}\tilde{t}} + Q = \sin(\tilde{t} + \phi) \quad \text{where } \alpha = 2\pi f (R_0 C t_0^{\mu})^{1/(1+\mu)} \tag{4}$$

is a dimensionless number that controls the behavior of the system. To determine the residual charge $Q(t = 0)$ on the droplet, we solved Eq. (4) numerically for fixed α and μ. $Q(t = 0)$ turns out to be distributed between 0 and its maximal value $Q_{\max} = \max_{\{\phi \in [0,2\pi]\}} Q(t = 0)$, depending on the value of ϕ. In Fig. 5 we plot $Q_{\max}$ as a function of α. Independent of the exact value of μ the droplets are found to discharge for $\alpha \gg 1$, whereas for $\alpha \leq 1$, $Q_{\max}$ approaches unity. The former leads to a contact angle after pinch off of $\theta \approx \theta_Y$, the latter to $\theta \approx \theta_L$, in agreement with the experimental observation. The former gives rise to fast regular oscillations (regime I), the latter to the slow contact angle relaxation after detachment (regime II). Equation (4) can also be used to fit the current in the system by varying α and ϕ using the previously determined value of μ (see Fig. 3). The fits and the experimental data are essentially indistinguishable. The corresponding values of α for a series of droplets with varying conductivity and viscosity are shown in the inset of Fig. 5. The expected linear dependence on f is confirmed within the experimental accuracy. Furthermore, the slope of the curves increases with increasing viscosity and decreases with increasing conductivity, as expected from the increase of t_0 with increasing η and decrease of R_0 with increasing σ.

In the case of the present electrowetting experiments, discharging of droplets during pinch off allows for the

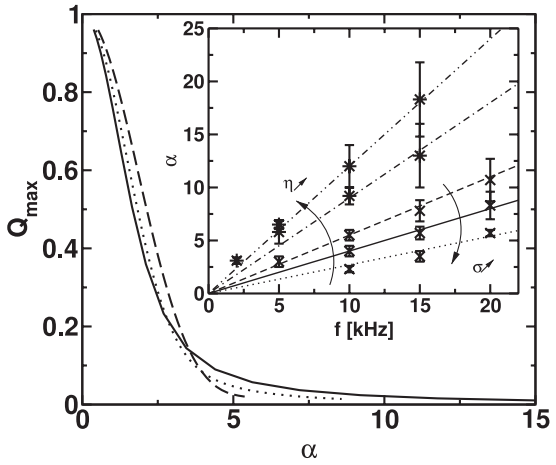

FIG. 5. Numerical results of the model: droplet charge after breakup vs α for various values of μ (dashed line $\mu = 3/2$, dots $\mu = 1$, full line $\mu = 2/3$). Inset: Values of α obtained from the fits of the electrical signal showing the linear behavior with the frequency for various viscosities ($\times 7$ mPa s; $*80$ mPa s) and conductivities (from top to bottom 1.0, 2.3, 0.8,1.8, 7.1 mS/cm).

occurrence of fast regular oscillations between the attached and the detached state. These oscillations can be used to promote mixing within liquid droplets, as currently under investigation in our group [2]. For millimeter sized droplets, mixing can be speeded up by 2 orders of magnitude in time compared to diffusion. However, the applicability of the mechanism presented here is much broader. Using the dimensionless parameter α the conditions for efficient droplet discharge can be predicted for arbitrary configurations in which droplets are created by using an electric field-induced instability of a liquid surface. In fact, existing designs of droplet generators for continuous ink-jet printing or for electrospraying have suitable dimensions to apply the discharging mechanism. An unresolved fundamental issue is the coupling between the electric fields and the hydrodynamics of the pinch off. The zoomed views of the capillary neck in Fig. 2(b) show the capillary neck immediately (≈ 60 μs) before the breakup. Obviously, the capillary neck becomes significantly longer in the low frequency case. Tentatively, we attribute this observation to the presence of stronger electric fields along the z axis at low frequency. This topic will be addressed in more detail in future work.

We thank Renate Nikopoulos, Udo Krafft, and Manfred Hörger for technical assistance. We are also indebted to Stephan Herminghaus and Michel Decré for fruitful discussions and comments on the manuscript. This work was supported by the German Science Foundation within the priority program Wetting and Structure Formation at Interfaces and by the Institute of Mechanics, Process, and Control Twente (IMPACT). J.-C. Baret acknowledges support by a Marie Curie Industry Host Contract No. IST-1999-80004.

*Author to whom correspondence should be addressed. Electronic address: f.mugele@tnw.utwente.nl

[1] A. A. Darhuber and S. M. Troian, Annu. Rev. Fluid Mech. **37**, 425 (2005).
[2] F. Mugele and J.-C. Baret, J. Phys. Condens. Matter **17**, R705 (2005).
[3] G. I. Taylor, Proc. R. Soc. A **280**, 383 (1964).
[4] J. B. Fenn, M. Mann, C. K. Meng, S. F. Wong, and C. M. Whitehouse, Science **246**, 64 (1989).
[5] L. Y. Yeo, D. Lastochkin, S.-C. Wang, and H.-C. Chang, Phys. Rev. Lett. **92**, 133902 (2004).
[6] J. M. Schneider, Recent Progress in Ink Jet Technology **II**, 246 (1999).
[7] J. Eggers, Rev. Mod. Phys. **69**, 865 (1997).
[8] J. R. Lister and H. A. Stone, Phys. Fluids **10**, 2758 (1998).
[9] J. Sagiv, J. Am. Chem. Soc. **102**, 92 (1980).
[10] J. W. S. Rayleigh, Proc. R. Soc. A **29**, 71 (1879).
[11] A. Klingner, S. Herminghaus, and F. Mugele, Appl. Phys. Lett. **82**, 4187 (2003).
[12] A. Klingner, J. Buehrle, and F. Mugele, Langmuir **20**, 6770 (2004).
[13] A detailed morphological diagram will be presented elsewhere. Baret and Mugele (to be published).
[14] During the short pinch off time, variations of the overall droplet geometry can be neglected. Thus $C = A_{sl}c$ is constant.
[15] J. C. Burton, J. E. Rutledge, and P. Taborek, Phys. Rev. Lett. **92**, 244505 (2004).
[16] J. D. Romano and R. H. Price, Am. J. Phys. **64**, 1150 (1996).
[17] Figure 4 shows also numerical results (solid lines) that were obtained using computational fluid dynamics calculations (CFD-ACE + package) using the volume of fluid method. Despite the known weakness of this type of calculation in the vicinity of singularities, the divergence of R agrees rather well with the experimental data. Details of these calculations that focus on the global droplet oscillation rather than the capillary breakup will be reported elsewhere.
[18] In air, $t_0 \sim (r_e^3\rho/\gamma)^{1/2} \approx 0.3$ ms in the inertia-dominated and $t_0 = \eta^3/\gamma^2\rho \approx 0.5$ ms in the viscosity-dominated case (see Ref. [7]).
[19] W. W. Zhang and J. R. Lister, Phys. Rev. Lett. **83**, 1151 (1999).
[20] I. Cohen, M. P. Brenner, J. Eggers, and S. R. Nagel, Phys. Rev. Lett. **83**, 1147 (1999).
[21] J. Eggers, Phys. Rev. Lett. **71**, 3458 (1993).
[22] See EPAPS Document No. E-PRLTAO-96-050604 for videos. This document can be reached via a direct link in the online article's HTML reference section or via the EPAPS homepage (http://www.aip.org/pubservs/epaps.html).